Adaptive evolution explains the present-day distribution of the thermal sensitivity of population growth rate

Dimitrios - Georgios Kontopoulos[1,2*], Thomas P. Smith[2], Timothy G. Barraclough[2], Samraat Pawar[2]

1 Science and Solutions for a Changing Planet DTP, Imperial College London, London, United Kingdom
2 Department of Life Sciences, Imperial College London, Silwood Park, Ascot, Berkshire, United Kingdom

* dgkontopoulos@gmail.com

Abstract

Developing a thorough understanding of how ectotherm physiology adapts to different thermal environments is of crucial importance, especially in the face of climate change. In particular, the study of how the relationship between trait performance and temperature (the "thermal performance curve"; TPC) evolves has been receiving increasing attention over the past years. A key aspect of the TPC is the thermal sensitivity, i.e., the rate at which trait values increase with temperature within temperature ranges typically experienced by the organism. For a given trait, the distribution of thermal sensitivity values across species is typically right-skewed. The mechanisms that underlie the shape of this distribution are hotly debated, ranging from strongly thermodynamically constrained evolution to adaptive evolution that can partly overcome thermodynamic constraints. Here we take a phylogenetic comparative approach and examine the evolution of the thermal sensitivity of population growth rate across phytoplankton and prokaryotes. We find that thermal sensitivity is moderately phylogenetically heritable and that the shape of its distribution is the outcome of frequent evolutionary convergence. More precisely, bursts of rapid evolution in thermal sensitivity can be detected throughout the phylogeny, increasing the amount of overlap among the distributions of thermal sensitivity of different clades. We obtain qualitatively similar results from evolutionary analyses of the thermal sensitivities of two underlying physiological traits, net photosynthesis rate and respiration rate of plants. Finally, we show that part of the variation in thermal sensitivity is driven by latitude, potentially as an adaptation to the magnitude of temperature fluctuations. Overall, our results indicate that adaptation can lead to large shifts in thermal sensitivity, suggesting that attention needs to be paid towards elucidating the implications of these evolutionary patterns for ecosystem function.

Author summary

Changes in environmental temperature influence the performance of biological traits (e.g., respiration rate) in ectotherms, with the relationship between trait performance and temperature (the "thermal performance curve") being single-peaked. Understanding how thermal performance curves adapt to different environments is important for predicting how organisms will be impacted by climate change. One key aspect of the

shape of these curves is the thermal sensitivity near temperatures typically experienced by the species. Currently, it remains unclear if thermal sensitivity can change through environmental adaptation or if it is nearly constant across environments. To address this question, in this study we use four datasets of thermal performance curves to reconstruct the evolution of thermal sensitivity across prokaryotes, phytoplankton, and plants. We show that thermal sensitivity does not evolve in a gradual manner, but can differ considerably even between closely related species. This suggests that thermal sensitivity undergoes rapid adaptive evolution, which is further supported by our finding that thermal sensitivity varies weakly with latitude. We conclude that variation in thermal sensitivity arises partly from adaptation to environmental factors and that this may need to be accounted for in ecophysiological models.

Introduction

According to current climate change projections, the average global temperature in 2100 is expected to be higher than the average of 1986-2005 by 0.3-4.8°C [1], coupled with an increase in temperature fluctuations in certain areas [2]. Therefore, it is now more important than ever to understand how temperature changes affect biological systems, from individuals to whole ecosystems. At the level of individual organisms, temperature affects ecological traits in the form of the "thermal performance curve" (TPC). Typically, this TPC, especially when the trait is a rate (e.g., respiration rate, photosynthesis, growth), takes the shape of a negatively-skewed unimodal curve (Fig. 1) [3,4]. The curve increases exponentially to a maximum (T_{pk}), and then also decreases exponentially, with the fall being steeper than the rise. Understanding how various aspects of the shape of this TPC adapt to a changing thermal environment is crucial for predicting how rapidly organisms can respond to climate change.

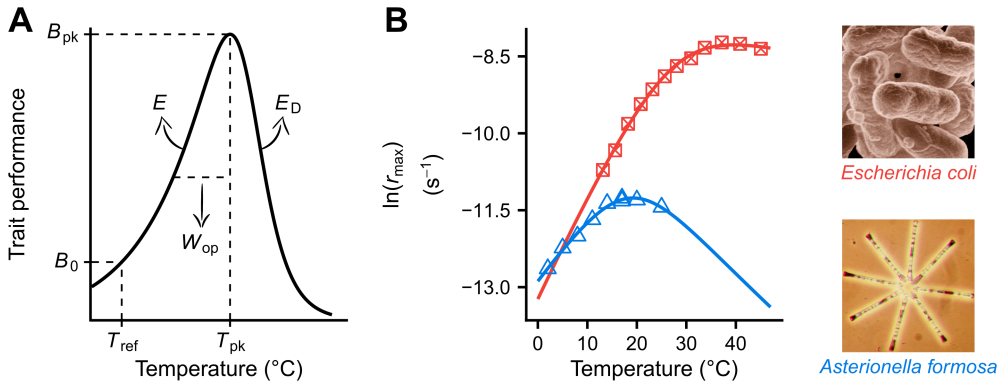

Fig 1. The thermal performance curve (TPC) of ectotherm metabolic traits, as described by the Sharpe-Schoolfield model [5]. (A) T_{pk} (K) is the temperature at which the curve peaks, reaching a maximum height that is equal to B_{pk} (in units of trait performance). E and E_{D} (eV) control how smoothly the TPC rises and falls respectively. B_0 (in units of trait performance) is approximately the trait performance normalised at a reference temperature (T_{ref}) below the peak. In addition, W_{op} (K), the operational niche width of the TPC, can also be calculated *a posteriori* as the difference between T_{pk} and the temperature at the rise of the TPC where $B(T) = 0.5 \cdot B_{\mathrm{pk}}$. (B) TPCs of r_{max} (and ecological traits in general) are usually well-described by the Sharpe-Schoolfield model.

Arguably the most popular theoretical framework that makes explicit predictions

about the influence of the environment on the shape of TPCs is the Metabolic Theory of Ecology (MTE) [6]. Within the original MTE framework [6–8], the shape of the TPC is expected to reflect the effects of temperature on the kinetics of a single rate-limiting enzyme involved in key metabolic reactions. Thus, according to the MTE, the exponential rise in trait values up to T_{pk} can be mechanistically described using the Boltzmann-Arrhenius equation:

$$B(T) = B_0 \cdot e^{\left[\frac{-E}{k} \cdot \left(\frac{1}{T} - \frac{1}{T_{\text{ref}}}\right)\right]}. \quad (1)$$

Here, B is the value of a biological trait, B_0 is a normalisation constant which gives the trait value at a reference temperature (T_{ref}), T is temperature (in K), k is the Boltzmann constant ($8.617{\cdot}10^{-5}$ eV $\cdot$ K^{-1}), and E (eV) is the thermal sensitivity of the trait within the temperature range typically experienced by the species or individual.

Early MTE studies argued that, because of strong thermodynamic constraints, adaptation will predominantly result in changes in B_0, whereas E will remain almost constant across traits (e.g., respiration rate, r_{max}), species, and environments around a range of 0.6-0.7 eV [6–8]. The latter assumption is referred to in the literature as the "universal temperature dependence" (UTD). The limited range of values that E can take is due to the average activation energy of respiration (≈ 0.65 eV), which is suggested to determine the shape of the TPCs of ecological traits. One notable exception to the UTD is net photosynthesis rate by plants whose TPCs should have a lower E value at ≈ 0.32 eV, similarly to the activation energy of photosynthesis [9].

The existence of a UTD has been hotly debated. From a theoretical standpoint, critics of the UTD have argued that the Boltzmann-Arrhenius model is too simple to mechanistically describe the complex physiological mechanisms of diverse organisms [3, 10–12]. These critics have argued that the model merely captures a statistical relationship between trait performance and temperature, emerging from the interaction of multiple factors (including evolutionary trade-offs with the local environment) and not solely from the effects of temperature on enzyme kinetics. As a result, the E calculated by fitting the Boltzmann-Arrhenius model to biological traits is an emergent property that does not directly reflect the activation energy of a single rate-limiting enzyme. For example, a fixed thermal sensitivity for net photosynthesis rate is not realistic because it depends on the rate of gross photosynthesis as well as photorespiration, which is in turn determined not only by temperature but also by the availability of CO_2 in relation to O_2 [13].

Indeed, there is now overwhelming empirical evidence for variation in E (thermal sensitivity) far exceeding the narrow 0.6-0.7 eV range [14–19]. Furthermore, the distribution of E values across species is not Gaussian but typically right-skewed. Given that E is necessarily positive (i.e., its lower boundary is 0 eV), a skewed distribution could, in theory, be due to measurement error around a fixed value of 0.65 eV [20]. In that case, however, we would expect a high density of E values close to 0 eV; such a pattern has not been observed [14]. Both the deviations from the theoretical expectation of 0.6-0.7 eV and the shape of the distribution of thermal sensitivity have been argued to be partly driven by adaptation to local environmental factors. These include selection on prey to have lower thermal sensitivity than predators (the "thermal life-dinner principle") [14], adaptation to temperature fluctuations [3, 21, 22], and adaptive increases in carbon allocation or use efficiency due to warming [23–26].

In general then, adaptive changes in the TPCs of underlying traits are expected to influence the TPCs of higher-order traits such as r_{max}, resulting in deviations from a UTD. Therefore, understanding how the thermal sensitivity of r_{max} and its distribution evolve is particularly important, as it may also yield useful insights about the evolution

of the TPCs of underlying physiological traits (e.g., respiration rate, photosynthesis rate, and carbon allocation efficiency). Indeed, systematic shifts in the thermal sensitivity of fundamental physiological traits have been documented, albeit not in a phylogenetic context. In particular, the phylogenetic heritability—the extent to which closely related species have more similar trait values than species chosen at random—of thermal sensitivity of $r_{\max}$ can provide key insights. Among phytoplankton, measures of thermal sensitivity of $r_{\max}$ (E and W_{op}) have previously been shown to exhibit intermediate phylogenetic heritability [27]. This indicates that among phytoplankton, thermal sensitivity is not constant but evolves along the phylogeny, albeit not as a purely random walk in trait space. To understand how variation in thermal sensitivity accumulates across diverse autotroph and heterotroph groups, in this study we conduct a thorough investigation of the evolutionary patterns of thermal sensitivity, focusing particularly on $r_{\max}$. Using a phylogenetic comparative approach, we test the following hypotheses:

1) **Thermal sensitivity does not evolve across species and any variation is noise-like.** This hypothesis agrees with the UTD concept described in early MTE studies. In this case, thermodynamic constraints would force E to be normally distributed, tightly around a mean of 0.65 eV (or 0.32 eV in the case of photosynthesis), with large deviations from the mean being mostly due to measurement error. If this hypothesis holds, thermal sensitivity would have zero phylogenetic heritability. We note, however, that the absence of phylogenetic heritability is not sufficient evidence on its own, as this could also be the outcome of a trait evolving extremely rapidly, to the point that its evolution is independent of the phylogeny.

2) **Thermal sensitivity evolves gradually across species but tends to revert to a global optimum trait value, without ever moving very far from it.** This hypothesis is also consistent with the UTD assumption, allowing for small deviations from an optimum. Such deviations may reflect adaptation to certain ecological lifestyles and, therefore, thermal sensitivity would be weakly phylogenetically heritable. Similarly to the previous hypothesis, thermodynamic constraints would prevent large deviations from the optimum.

3) **Thermal sensitivity evolves in other ways.** This is an "umbrella" hypothesis that encompasses sub-hypotheses that do not invoke the UTD assumption. For example, a global optimum may still exist, but its influence would be very weak, allowing for a wide exploration of the parameter space away from it. In this case, changes in thermal sensitivity would be the outcome of adaptation to different thermal environments. Another sub-hypothesis may posit that clades differ systematically in the rate at which thermal sensitivity evolves, due to the occasional emergence of evolutionary innovations. Thus, clades with high evolutionary rates would be able to better explore the parameter space of thermal sensitivity (i.e., through large changes in E and W_{op} values), compared to low-rate clades in which thermal sensitivity would evolve more gradually. A third possible sub-hypothesis is that evolution may favour species that are increasingly independent of temperature changes. In that case, the global optimum of E would not be stationary, but moving towards lower values with time. It is worth clarifying that these three sub-hypotheses are not necessarily mutually exclusive.

Results

We used four TPC datasets: i) $r_{\max}$ across 380 phytoplankton species [27], ii) $r_{\max}$ across 272 prokaryote species [28], iii) net photosynthesis rates across 221 species of

algae, aquatic and terrestrial plants [26], and iv) respiration rates across 201 species of algae, aquatic and terrestrial plants [26]. Trait values were typically measured under nutrient-, light- and CO_2-saturated conditions (where applicable), after acclimation to each experimental temperature.

Phylogeny reconstruction

To investigate the evolution of measures of thermal sensitivity across species, we reconstructed the phylogeny of as many species in the four datasets as possible. We collected publicly available nucleotide sequences of i) the small subunit rRNA gene from all species groups and the ii) cbbL/rbcL gene from photosynthetic prokaryotes, algae, and plants. We managed to obtain small subunit rRNA gene sequences from 537 species and cbbL/rbcL sequences from 208 of them (Tables S3 and S4 in the S1 Appendix). Sequence alignment was conducted using MAFFT (v. 7.123b) [29] and its L-INS-i algorithm. We then performed masking by running Noisy (v. 1.5.12) [30] with the default options to remove phylogenetically uninformative homoplastic sites.

For a more robust phylogenetic reconstruction, we used the results of previous phylogenetic studies by extracting the Open Tree of Life [31] topology for the species in our dataset using the rotl R package [32]. We manually examined the topology to eliminate any obvious errors. In total, 497 species were present in the tree, whereas many nodes were polytomic. To add missing species and resolve polytomies, we inferred 1,500 trees with RAxML (v. 8.2.9) [33] from our concatenated sequence alignment, using the Open Tree of Life topology as a backbone constraint. Finally, we calibrated the RAxML tree with the highest log-likelihood to units of relative time by running DPPDiv [34] on the alignment of the small subunit rRNA gene sequences using the uncorrelated Γ-distributed rates model [35] (Fig. S1 in the S1 Appendix).

Estimation of TPC parameters

To quantify the parameters (including E and W_{op}) of each experimentally determined TPC, we fitted the following four-parameter variant of the Sharpe-Schoolfield model (Fig. 1) [5, 27]:

$$B(T) = B_0 \cdot \frac{e^{\left[\frac{-E}{k}\cdot\left(\frac{1}{T}-\frac{1}{T_{\mathrm{ref}}}\right)\right]}}{1+\frac{E}{E_{\mathrm{D}}-E}\cdot e^{\left[\frac{E_{\mathrm{D}}}{k}\cdot\left(\frac{1}{T_{\mathrm{pk}}}-\frac{1}{T}\right)\right]}}. \quad (2)$$

This model extends the Boltzmann-Arrhenius model (Eq. 1) to capture the decline in trait performance after the TPC reaches its peak (T_{pk}). After rejecting fits with an R^2 below 0.5, there were i) 312 fits across 118 species from the phytoplankton r_{max} dataset, ii) 289 fits across 189 species from the prokaryote r_{max} dataset, iii) 87 fits across 38 species from the net photosynthesis rates dataset, and iv) 34 fits across 18 species from the respiration rates dataset. Note that some species were represented by multiple fits due to the inclusion of experimentally-determined TPCs from different strains of the same species or from different geographical locations. Further filtering was performed to ensure that each TPC parameter per fit was robustly estimated (see the Methods section).

The inferred estimates of thermal sensitivity were not normally distributed but were skewed to the right (Fig. S2 in Appendix S1), similarly to previous studies [14, 16]. Furthermore, we did not detect a disproportionately high density of thermal sensitivity

values near the lower boundary of E (0 eV), as we would expect if all variation was due to measurement error around a true value of e.g., 0.65 eV. Thus, these results are not consistent with the hypothesis of a fixed thermal sensitivity (hypothesis 1).

Phylogenetic comparative analyses

To further test our three hypotheses, we next examined the evolutionary patterns of thermal sensitivity. Given that the main focus of this study is to investigate how the thermal sensitivity of $r_{\max}$ (a higher-order trait) evolves, most of the following comparative analyses were performed on our two large TPC datasets ($r_{\max}$ of phytoplankton and prokaryotes). Besides this, the sample sizes of the two smaller datasets would be inadequate for obtaining robust results for many of our analyses. If an analysis makes use of all four datasets, this is explicitly stated.

An issue that is worth mentioning is the overlap between the datasets of phytoplankton and prokaryotic TPCs, given that phytoplankton are a polyphyletic group which includes Cyanobacteria. To address this, we kept Cyanobacteria as part of the phytoplankton dataset (due to their functional similarity) and did not include them in analyses of prokaryotes. We also examined whether our results were mainly driven by the long evolutionary distance between Cyanobacteria and eukaryotic phytoplankton by repeating all phytoplankton analyses after removing Cyanobacteria (see subsection S3.2 in Appendix S1).

Phylogenetic heritability estimation

The phylogenetic heritability of a continuous trait is a measure of the contribution of the phylogeny to the distribution of present-day trait values [36]. A phylogenetic heritability of 1 indicates that the trait evolves randomly, according to Brownian motion. In contrast, a phylogenetic heritability of 0 is evidence that trait values are independent of the phylogeny, either because i) the trait is practically invariant across species and any variation is due to measurement error or because ii) the evolution of the trait is very fast and with frequent convergence. Phylogenetic heritabilities between 0 and 1 reflect deviations from random evolution (e.g., due to occasional patterns of evolutionary convergence).

As TPC parameters capture different aspects of the shape of the same curve, it is likely that some of them may covary [27]. To account for this in the estimation of phylogenetic heritability, we fitted a multi-response phylogenetic model using the MCMCglmm R package (v. 2.26) [37] in which all TPC parameters formed a combined response. The model was fitted separately to our two large TPC datasets: $r_{\max}$ of phytoplankton and prokaryotes. To satisfy the assumption of models of trait evolution that the change in trait values is normally distributed, we transformed all TPC parameters so that their distributions would be approximately Gaussian (see Fig. 2). To integrate the inverse of the phylogenetic variance/covariance matrix into each model, we first pruned our tree and obtained subtrees that only included species for which data were available.

Non-negligible phylogenetic heritability was detected in thermal sensitivity measures, as well as all other TPC parameters, across phytoplankton (including or excluding Cyanobacteria) and prokaryotes (Figs. 2 and S7). In particular, the phylogenetic heritability estimates of $\ln(E)$ and $\ln(W_{\text{op}})$ were statistically different from both zero and one, indicating that the two TPC parameters evolve across the phylogeny but not in a purely random Brownian manner. Based on these results, the hypothesis that thermal sensitivity does not vary across species (hypothesis 1) can clearly be rejected.

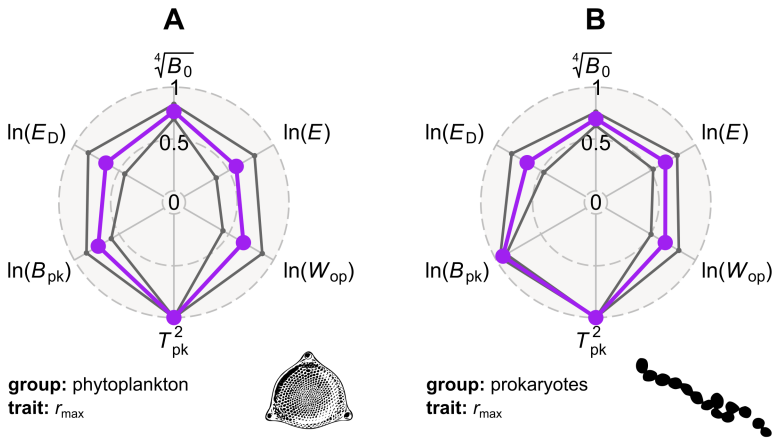

Fig 2. Moderate to strong phylogenetic heritability can be detected in all TPC parameters, across phytoplankton and prokaryotes. The three circles of each radar chart correspond to phylogenetic heritabilities of 0, 0.5, and 1. Mean phylogenetic heritability estimates are shown in purple, whereas the 95% HPD intervals are in dark grey. Note that we statistically transformed all TPC parameters so that their distributions would be approximately Gaussian. In general, TPC parameters exhibit similar phylogenetic heritability between the two species groups. The only major exception is $\ln(B_{pk})$, which is considerably more heritable among prokaryotes than among phytoplankton. This difference in phylogenetic heritability most likely reflects the strength of the positive correlation between B_{pk} and T_{pk} in the two groups. More precisely, T_{pk}, which has a phylogenetic heritability of ≈ 1, is more strongly correlated with B_{pk} among prokaryotes [28] than among phytoplankton [27], possibly due to differences in their cellular physiology. As a result, the phylogenetic heritability of $\ln(B_{pk})$ in prokaryotes is very close to that of T^2_{pk}.

Partitioning of thermal sensitivity across the phylogeny

To understand why thermal sensitivity has an intermediate phylogenetic heritability, we examined how clades throughout the phylogeny explore the parameter space. For this, we used a disparity-through-time analysis [38, 39]. At each branching point of the phylogeny, mean subclade disparity is calculated as the average squared Euclidean distance among trait values within the subclades, normalised to the disparity of trait values across the entire tree. The resulting disparity line is then compared to the null expectation, i.e., an envelope of disparities obtained from simulations of random evolution on the same tree. Through the comparison of the true trait disparity with the null expectation, it is possible to identify the exact periods of evolutionary time during which mean subclade disparity is higher or lower than expected under random evolution. Higher than expected subclade disparity indicates that clades converge in trait space, whereas lower than expected subclade disparity suggests that clades occupy distinct areas of parameter space (adaptive radiation) due to a deceleration of the evolutionary rate. Such patterns would be consistent with hypothesis 3.

We performed disparity-through-time analyses for $\ln(E)$ and $\ln(W_{op})$, using the rank envelope method [39] to generate a confidence envelope from 10,000 simulations of random evolution. As it is not straightforward to incorporate multiple measurements per species with this method, we selected the $\ln(E)$ or $\ln(W_{op})$ estimate of the Sharpe-Schoolfield fit with the highest R^2 value per species. We note that the ideal approach would be to estimate the median $\ln(E)$ and $\ln(W_{op})$ value for each species from large intraspecific samples. This was not possible, however, as for almost all

species we had one or very few intraspecific estimates. The mean subclade disparity of thermal sensitivity measures was higher than expected near the present, highlighting an increasing overlap in the parameter space of thermal sensitivity among distinct clades (Figs. 3 and S8). This pattern of increasing clade-wide convergence in thermal sensitivity is also easily apparent through the comparison of thermal sensitivity distributions among large phyla (Figs. 4 and S3).

Mapping the evolutionary rate on the phylogeny

We next investigated if clades systematically differ in their evolutionary rate of thermal sensitivity (part of hypothesis 3). To this end, we estimated the evolutionary rate of thermal sensitivity measures for each branch of the phylogeny by fitting two extensions of the Brownian motion model: the free model [40] and the stable model [41]. Under the free model, the trait undergoes random evolution but with an evolutionary rate that varies across branches. The stable model can be seen as a generalisation of the free model, as the evolutionary change in trait values is sampled from a heavy-tailed stable distribution, of which the Gaussian distribution (assumed under Brownian motion) is a special case. Thus, the stable model should provide a more accurate representation of evolutionary rate variation, as it is better able to accommodate jumps in parameter space towards rare and extreme trait values.

The results were robust to the choice of model used for inferring evolutionary rates (Figs. 5 and S5). Rate shifts tend to occur sporadically throughout the phylogeny and especially in late-branching lineages, without being limited to particular clades. This pattern suggests that there is little variation in the evolutionary rate of thermal sensitivity among clades, with sudden bursts of trait evolution arising in parallel across evolutionarily remote lineages.

Visualization of trait evolution as a function of time and test for directional selection

To further describe the evolution of thermal sensitivity, we visualized the E and W_{op} values from the root of each subtree until the present day, across all four TPC datasets. Ancestral states – and the uncertainty around them – were obtained from fits of the stable model of trait evolution, as described in the previous subsection. The visualization allowed us to test hypothesis 2, i.e., that thermal sensitivity evolves closely around an optimum value, with large deviations from the optimum quickly reverting back to it. To also test the MTE expectation of a global optimum around 0.65/0.32 eV for E (hypothesis 2), as well as the hypothesis of directional selection towards lower thermal sensitivity (part of hypothesis 3), we used the following model:

$$\ln(E) \sim \ln(\widehat{\theta}) + \mathrm{slope} \cdot t. \tag{3}$$

$\ln(E)$ values (those from extant species and ancestral states inferred with the stable model) were regressed against a global optimum ($\ln(\widehat{\theta})$) and a slope that captures a putative linear trend towards lower/higher values with relative time, t. The same model was also fitted to $\ln(W_{\mathrm{op}})$. The regressions were performed with MCMCglmm and were corrected for phylogeny as this resulted in lower Deviance Information Criterion (DIC) [42] values than those obtained from non-phylogenetic variants of the models. More precisely, we executed two MCMCglmm chains per regression for a million generations, sampling every thousand generations after the first hundred thousand.

The aforementioned analysis (Fig. 6) did not provide support for the hypothesis of strongly constrained evolution around a single global optimum (hypothesis 2). Instead, lineages explore large parts of the parameter space, often moving rapidly towards the

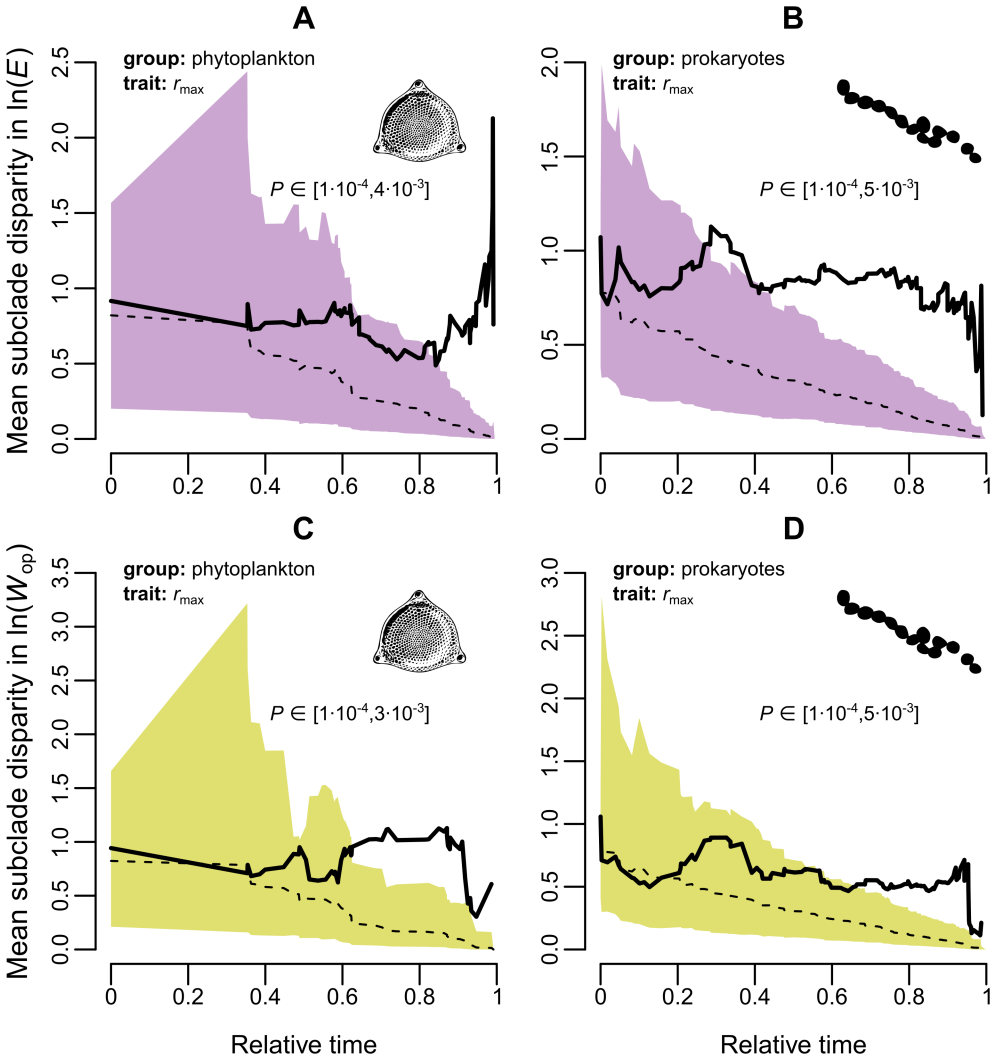

Fig 3. The mean subclade disparity in thermal sensitivity tends to exceed that expected under random evolution, given enough time. Shaded regions represent the 95% confidence interval of the resulting trait disparity from 10,000 simulations of random Brownian evolution on each respective subtree. The dashed line stands for the median disparity across simulations, whereas the solid line is the observed trait disparity. The latter is plotted from the root of the tree ($t = 0$) until the most recent internal node. The reported P-values were obtained from the rank envelope test, whose null hypothesis is that the trait undergoes random evolution. Note that instead of a single value, a range of P-values is produced for each panel, due to the existence of ties. A general pattern emerges, indicating that species from evolutionary remote clades tend to increasingly overlap in thermal sensitivity space with time.

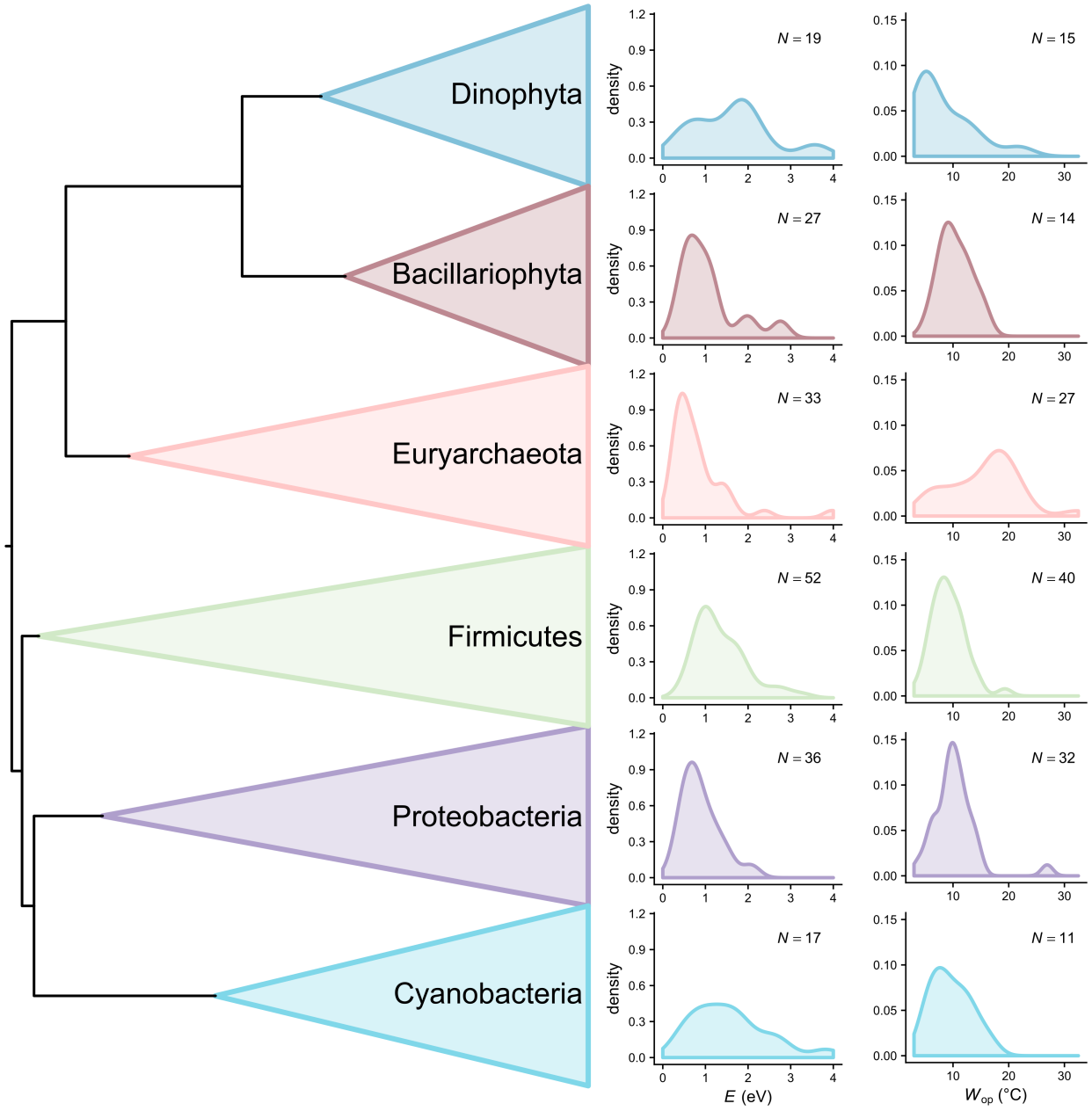

Fig 4. Distributions of thermal sensitivity estimates of r_{max} for the largest phyla of this study. In general, more variation can be observed within than among phyla. For example, E and W_{op} are similarly distributed among Proteobacteria and Bacillariophyta despite the long evolutionary distance that separates the two phyla. This high amount of convergence in thermal sensitivity space by diverse lineages suggests that variation in the two TPC parameters is mainly driven by adaptation to local environmental conditions, irrespective of species' evolutionary history. In other words, it is likely that particular thermal strategies (e.g., having low thermal sensitivity) may yield significant fitness gains at certain environments (e.g., those with large temperature fluctuations), leading to convergent evolution of thermal sensitivity.

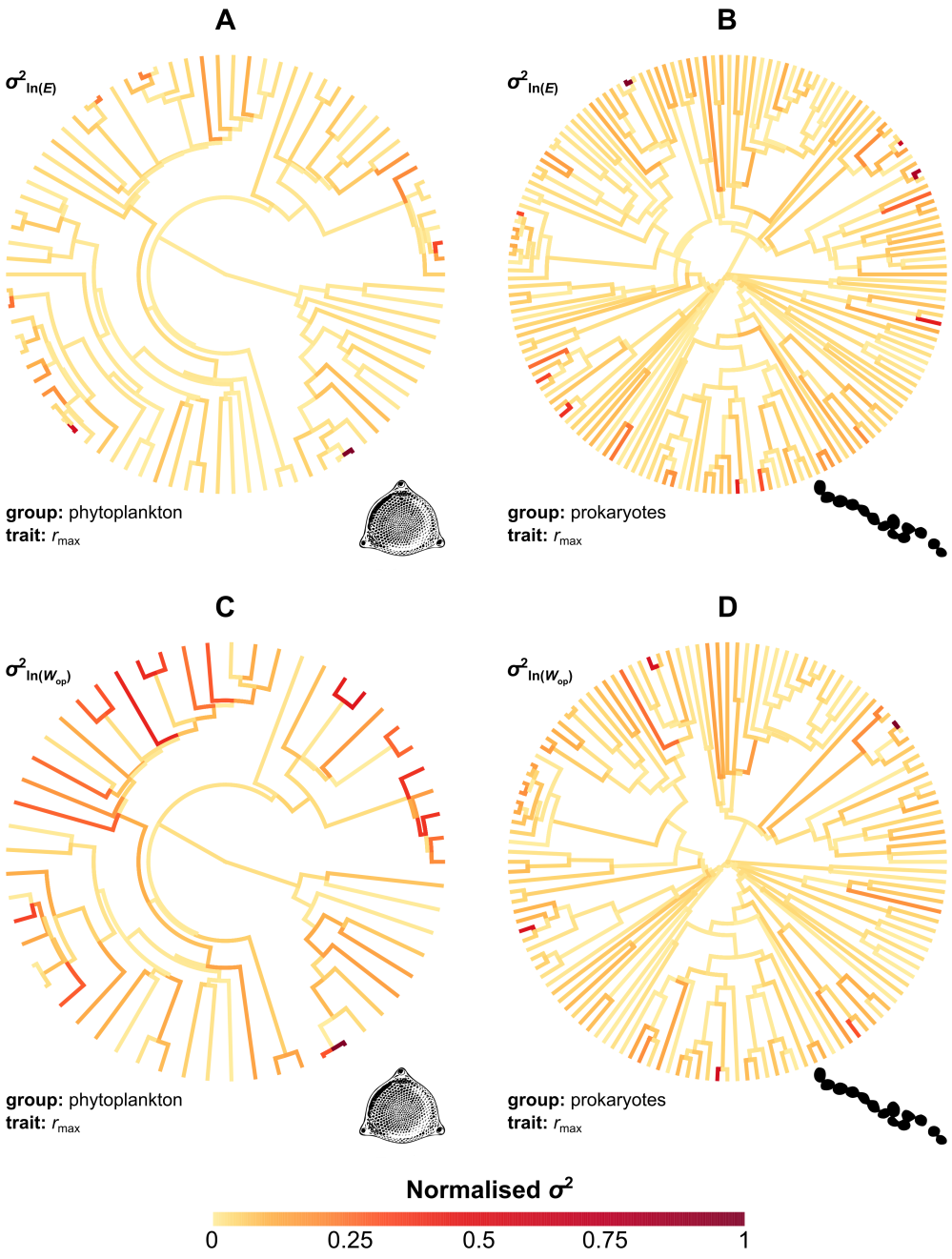

Fig 5. Variation in the evolutionary rate of thermal sensitivity across the phylogeny. Rates were estimated by fitting the stable model of trait evolution to each dataset and were then normalised between 0 and 1. Most branches exhibit relatively low rates of evolution (orange), whereas the highest rates (red and brown) are generally observed in late-branching lineages across different clades.

upper and lower bounds (i.e., 0 and 4 eV), without reverting back to the presumed optimum (e.g., see the clade denoted by the arrow in Fig. 6D). The estimated optima for E of the two r_{max} datasets were much higher than 0.65 eV and, in the case of prokaryotes (Fig. 6B), the 95% HPD interval did not include 0.65. Similarly, the inferred optimum values for E of net photosynthesis rate and respiration rate (0.52 eV and 2.06 eV respectively; Fig. S9A,B) were both higher than the theoretical expectations of 0.32 and 0.65 eV. The slope parameter that would capture any directional trend in thermal sensitivity (part of hypothesis 3) was not statistically different from zero for any dataset.

Latitudinally structured variation in thermal sensitivity

All our analyses in this study so far appear to converge on one conclusion: that the evolution of thermal sensitivity can be rapid and largely independent of the evolutionary history of each lineage. This suggests that certain environments may select for particular values of thermal sensitivity. To identify environmental adaptation in thermal sensitivity, we examined whether it varies with latitude across the combination of all four TPC datasets. A latitudinal relationship could suggest that thermal sensitivity changes in response to temperature fluctuations. In this case, we would expect selection for thermal specialists near the equator where temperature fluctuations are low and an increasing trend towards thermal generalists at higher latitudes. In support of this hypothesis, the E values of phytoplankton r_{max} have been previously shown to decrease from the equator to mid-latitudes [27].

The best-fitting models revealed that latitude indeed explains some variation in E but not in W_{op} (Figs. 7 and S10, Tables S1 and S2). The E estimates of r_{max}, net photosynthesis rate, and respiration rate differed statistically in their intercepts but not in their slopes against latitude, although the latter could be an artefact of the small sample size. This result suggests that latitude could influence the E values of not only r_{max} but also other traits across various species groups.

Discussion

In this study, we have performed a thorough analysis of the evolution of the thermal sensitivities of r_{max} and its two key underlying physiological traits (net photosynthesis rate and respiration rate). To achieve this, we formulated and tested three alternative hypotheses that capture different views expressed in the literature regarding the impact of thermodynamic constraints on the evolution of two measures of thermal sensitivity: E and W_{op} (Fig. 1).

The first hypothesis is that thermal sensitivity is strictly constant across traits, species, and environments, as it is directly determined by the activity of a single key rate-limiting enzyme involved in metabolic reactions. This hypothesis was first introduced in early papers that described the Metabolic Theory of Ecology [6–8]. We did not find support for this hypothesis as we detected substantial variation in thermal sensitivity (Fig. S2 in the S1 Appendix), which was also found to be phylogenetically heritable among phytoplankton and prokaryotes (Fig. 2).

Our second hypothesis can be thought of as a relaxed version of the first. According to it, thermal sensitivity is able to evolve, but only close to an "optimum" value due to strong (but not completely insurmountable) thermodynamic constraints. We tested this hypothesis using a series of phylogenetic comparative analyses. These analyses showed that the evolution of thermal sensitivity is characterised by an increasing overlap in parameter space by evolutionarily remote lineages (Figs. 3 and 4) due to bursts of rapid evolution (Fig. 5). Additionally, visualisation of thermal sensitivity evolution through

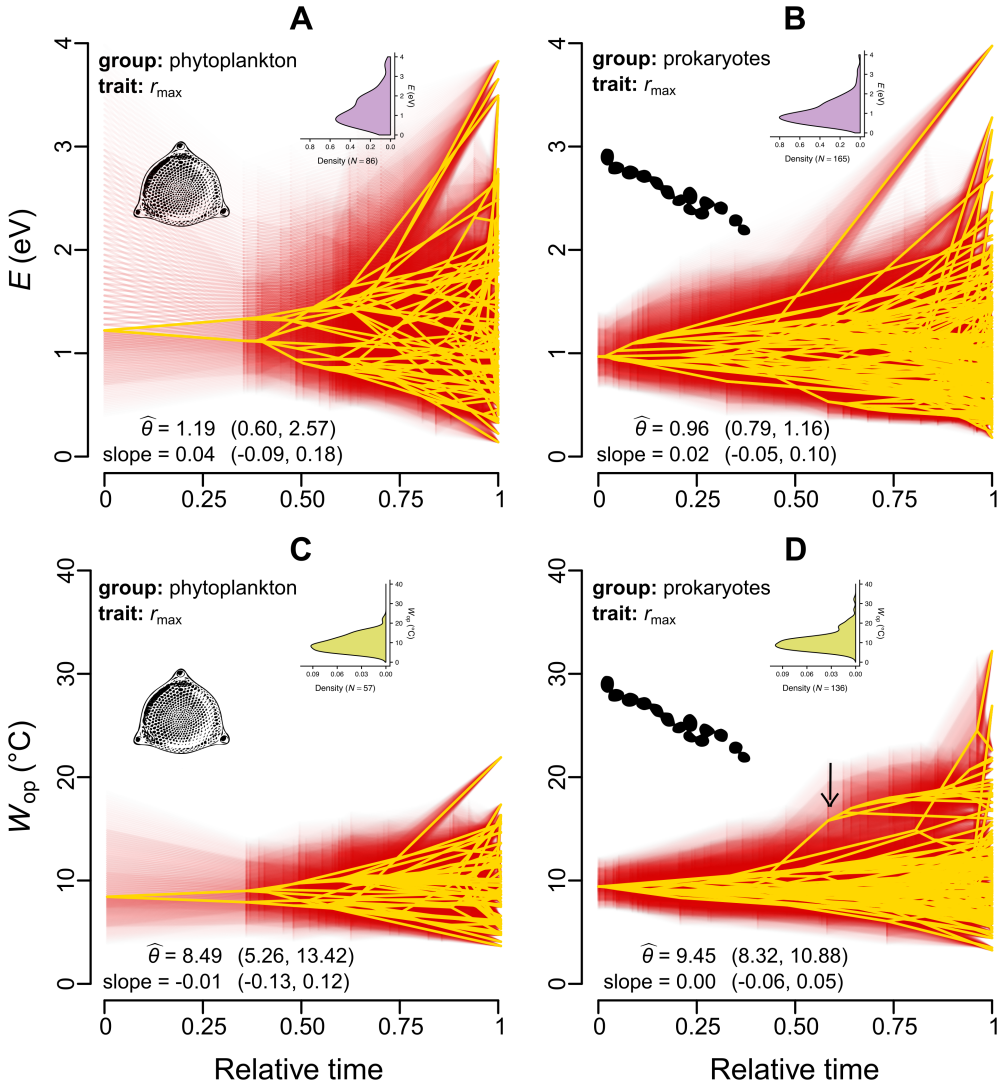

Fig 6. Projection of the phylogeny into thermal sensitivity versus time space. The values of ancestral nodes were estimated from fits of the stable model. Yellow lines represent the median estimates, whereas the 95% credible intervals are shown in red. $\widehat{\theta}$ is the estimated global optimum for each panel, whereas the existence of a linear trend towards lower/higher values is captured by the reported slope. Parentheses stand for the 95% HPD intervals for $\widehat{\theta}$ and the slope. All estimates were obtained for $\ln(E)$ and $\ln(W_{op})$, but the parameters are shown here in linear scale. The inset figures show the density distributions of E and W_{op} values of extant species in the dataset. The arrow in panel D shows an example of a whole clade shifting towards high W_{op} values, without being attracted back to $\widehat{\theta}$.

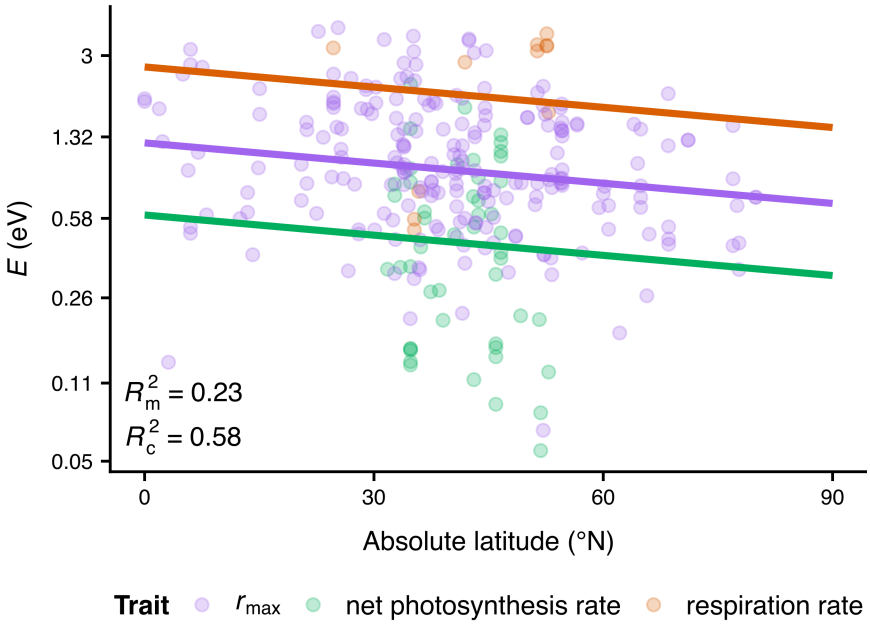

Fig 7. E values weakly decrease with absolute latitude. A possible driver of this pattern could be the increase in temperature fluctuations from low to high latitudes, resulting in stronger selection pressure for thermal generalists (with lower E values). 23% of the variance is explained by latitude and trait identity, whereas the addition of species identity as a random effect on the intercept raises the amount of explained variance to 58%. Note that values on the vertical axis increase exponentially.

time (Figs. 6 and S9) showed that thermal sensitivity can rapidly move away from its presumed optimum value without being strongly attracted back to it (e.g., see the arrow in Fig. 6D). These results are inconsistent with the hypothesis that strong thermodynamic constraints prevent large shifts in thermal sensitivity away from a global optimum (hypothesis 2).

Our final hypothesis was that thermal sensitivity evolves in an adaptive manner and that even if a global optimum exists, its influence on thermal sensitivity evolution is very weak. This hypothesis was supported both by our analyses of trait macroevolution and by a detected relationship between E and latitude (Fig. 7). The latter result agrees with the expectation that thermally variable environments should impose selection for phenotypes with low thermal sensitivity, and vice versa [3, 21]. However, a latitudinal relationship could not be detected for W_{op}. One possible interpretation for this result is that the smaller sample of W_{op} values did not permit the recognition of a latitudinal association. Alternatively, and given the nonlinearity in the rising part of the TPC, it is possible that E is a more meaningful measure of thermal sensitivity than W_{op}. While the latter implicitly assumes that species experience temperatures close to T_{pk}, E is able to capture the thermal sensitivity across the entire rise of the TPC.

In light of these results, a mechanistic interpretation of TPC evolution can be derived from the comparison of phylogenetic heritabilities of TPC parameters (Fig. 2). Contrary to E and W_{op} which have intermediate phylogenetic heritabilities, T_{pk} is almost perfectly phylogenetically heritable and evolves relatively gradually (i.e., large jumps in parameter space cannot be observed; see Fig. S6 in the S1 Appendix). Thus, we expect TPCs to adapt to different thermal environments through both slight changes in T_{pk} and larger changes in E. Fundamental differences in the selection mechanisms underlying the evolution of these two parameters may explain this key difference in

evolutionary patterns between them. Specifically, while T_{pk} and E are both associated with latitude, the former responds to mean environmental temperature [27, 43] while the latter to temperature fluctuations [3, 21, 22, 27]. We hypothesize that a species adapted to low temperatures is unlikely to adapt to a high-temperature environment rapidly enough (i.e., through a large increase in T_{pk}) as it is pushed to its thermal tolerance limits [44, 45]. In contrast, a species adapted to a fluctuating thermal environment (i.e., having a low E value) should be able to survive in more thermally stable conditions and eventually become a thermal specialist (with a high E value). Nevertheless, latitude, trait identity, and species identity account for only 58% of the variance in E (Fig. 7), indicating that shifts in E may also be driven by other factors such as biotic interactions [14, 46, 47]. A systematic identification of drivers of thermal sensitivity as well as the magnitude of their respective influence could be the focus of future studies.

For the thermal sensitivity of r_{max} in particular, the observed patterns of non-gradual evolution could partly reflect the evolution of the TPCs of underlying physiological traits on which r_{max} depends (e.g., photosynthesis rate and respiration rate in phytoplankton). More precisely, it is possible that even moderate changes in the TPCs of fundamental traits could have, in combination, strong knock-on effects on the thermal sensitivity of r_{max} [23]. In support of this, we have previously shown that in populations of photosynthetic cells, shifts in the thermal sensitivity of carbon allocation efficiency will necessarily induce changes in the thermal sensitivity of r_{max} [26]. Further research is clearly needed to identify how different traits and their thermal sensitivities interact, and the extent to which such interactions can be modified through adaptation. Nonetheless, it is worth emphasising that large adaptive shifts in thermal sensitivity can be observed even for fundamental physiological traits such as respiration rate (Fig. S9B,D), contrary to the MTE expectation of strong evolutionary conservatism [6–8]. It remains to be seen whether this pattern reflects a similar lack of evolutionary conservation in the shape of the thermal stability curves [48] of enzymes involved in metabolic reactions.

Besides variation in thermal sensitivity that has a biological basis, "artificial" variation may also be present, hindering the recognition of real patterns. For example, E estimates can be inaccurate if trait measurements at the rise of the TPC are limited and only span a narrow range of temperatures [17]. To prevent this issue, we only kept E estimates if at least four trait measurements were available at the rise of each TPC. Further variation in thermal sensitivity can be introduced if trait values are measured instantaneously (without allowing sufficient time for acclimation) or under suboptimal conditions (e.g., under nutrient- or light-deficient conditions). Such treatments can lead to systematic biases in the shape of the resulting TPCs, which may strongly differ from TPCs obtained after adequate acclimation and under optimal growth conditions [23, 49–52]. Regarding our study, the datasets that we used only included TPCs that were experimentally determined after acclimation and under optimal conditions.

In any case, it is worth stressing that TPC adaptation is generally associated in the ecological literature with shifts in T_{pk} or B_{pk} and less so with changes in thermal sensitivity [3]. A possible explanation for this is that the mechanisms that could lead to changes in E may occur under more complex selective environments or longer timescales than those in most evolutionary ecology experiments. In particular, gradual changes in T_{pk} may be achieved through evolutionary shifts in the melting temperature of enzymes, i.e., the temperature at which 50% of the enzyme population is deactivated [48, 53]. In contrast, changes in thermal sensitivity may be the outcome of i) evolution of enzymes with different heat capacities [48, 54, 55], ii) changes in the plasticity of cellular membranes [3, 56], or even iii) restructuring of the underlying metabolic network [57].

Overall, our results emphasize the need to consider variation in E, as has been

pointed out before [14, 16, 17, 26]. In particular, a number of studies had previously identified right skewness in the E distributions of multiple traits and taxonomic groups [14, 16, 17]. However, a clear explanation for this pattern was lacking, given that E was expected to be strongly thermodynamically constrained and thus almost invariable across species [6–8]. Our study fills this gap by showing that the distribution of E is the outcome of frequent convergent evolution, driven by the adaptation of species from different clades to similar environmental conditions. In other words, as species encounter new environments through active or passive dispersal [58–60], they face selection for particular values of thermal sensitivity, which often results in large shifts in E. This process explains both the low variation in E among species groups (Fig. 4) and the shape of its distribution. More precisely, the high degree of right skewness probably reflects the fact that most environments select for thermal generalists, with high E values being less frequently advantageous. Our findings have implications for ecophysiological models which may benefit from accounting for variation in thermal sensitivity among species or individuals. This could both yield an improved fit to empirical datasets [61] and provide a more realistic approximation of the processes being studied. Finally, the existence of adaptive variation in thermal sensitivity is likely to partly drive ecological patterns at higher scales (e.g., the response of an ecosystem to warming). How differences in thermal sensitivity among species influence ecosystem function is largely unaddressed [28, 61] but highly important for accurately predicting the impacts of climate change on diverse ecosystems.

Methods

Phylogeny reconstruction and relative time calibration

We specified the General Time-Reversible model [62] with Γ-distributed rate variation among sites [63] as the evolutionary model in RAxML. The topology was kept fixed between the two gene partitions (i.e., one partition for the alignment of the small subunit rRNA gene sequences and one partition for the alignment of cbbL/rbcL gene sequences), whereas the parameters of the evolutionary model were allowed to differ. Out of the 1,500 resulting tree topologies, we selected the tree with the highest log-likelihood and performed bootstrapping (using the extended majority-rule criterion) [64] to evaluate the statistical support for each node.

For time calibration, we used the alignment of small subunit rRNA gene sequences only, as DPPDiv can only be run on a single gene partition. We executed two DPPDiv runs for 9.5 million generations, sampling from the posterior distribution every 100 generations. After discarding the first 25% of samples as burn-in, we ensured that the two runs had converged on statistically indistinguishable posterior distributions by examining the effective sample size and the potential scale reduction factor [65, 66] for all model parameters. More precisely, we verified that all parameters had an effective sample size above 200 and a potential scale reduction factor value below 1.1. To summarise the posterior distribution of calibrated trees into a single relative chronogram, we kept 4,750 trees per run (one tree every 1,500 generations) and calculated the median height for each node using the TreeAnnotator program [67].

Sharpe-Schoolfield model fitting

We followed the same approach for fitting the Sharpe-Schoolfield model as in reference [27]. Briefly, we set T_{ref} to 0°C, as for B_0 to be biologically meaningful (see Fig. 1), it needs to be normalised at a temperature below the minimum T_{pk} in the study. Thus, a T_{ref} value of 0°C allowed us to include TPCs from species with low T_{pk}

values in the analyses. Also, as certain specific TPC parameter combinations can mathematically lead to an overestimation of B_0 compared to the true value, $B(T_{\mathrm{ref}})$ [68], we manually recalculated $B(T_{\mathrm{ref}})$ for each TPC after obtaining estimates of the four main parameters (B_0, E, T_{pk}, and E_{D}). For simplicity, these recalculated $B(T_{\mathrm{ref}})$ values are referred to as B_0 throughout the study. Finally, B_{pk} and W_{op} were calculated based on the estimates of the four main parameters.

To ensure that all TPC parameters were reliably estimated, we filtered the resulting estimates based on the following criteria: i) B_0 and E estimates were rejected if fewer than four experimental data points were available below T_{pk}. ii) Extremely high E estimates (i.e., above 4 eV) were rejected. iii) W_{op} values were retained if at least four data points were available below T_{pk} and two after it. iv) Two data points below and after the peak were required for accepting the estimates of T_{pk} and B_{pk}. v) E_{D} estimates were kept if at least four data points were available at temperatures greater than T_{pk}.

Estimation of phylogenetic heritability for all TPC parameters

As in the previous subsection, the methodology that we used here was identical to that in reference [27]. In short, we specified a phylogenetic mixed-effects model for each of the two large TPC datasets with MCMCglmm. The models had a combined response with all TPC parameters transformed towards normality. The uncertainty for each estimate was obtained with the delta method [69] or via bootstrapping (for $\ln(W_{\mathrm{op}})$) and was incorporated into the model. Missing estimates in the response variables (i.e., when not all parameter estimates could be obtained for the same TPC) were modelled according to the "Missing At Random" approach [36,37]. Regarding fixed effects, a separate intercept was specified for each TPC parameter. Species identity was treated as a random effect on the intercepts and was corrected for phylogeny through the integration of the inverse of the phylogenetic variance/covariance matrix. For each dataset, two Markov chain Monte Carlo chains were run for 200 million generations and estimates of the parameters of the model were sampled every 1,000 generations after the first 20 million generations were discarded as burn-in. Tests to ensure that the chains had converged and that the parameters were adequately sampled were done as previously described.

Free and stable model fitting

We fitted the free and the stable models of trait evolution to estimates of $\ln(E)$ and $\ln(W_{\mathrm{op}})$, using the motmot.2.0 R package (v. 1.1.2) [70,71] and the stabletraits software [41] respectively. To obtain each fit of the stable model, we executed four independent Markov chain Monte Carlo chains for 30 million generations, recording posterior parameter samples every 100 generations. Samples from the first 7.5 million generations were excluded, whereas the remaining samples were examined to ensure that convergence had been achieved.

Investigation of a putative relationship between latitude and $\ln(E)$ and $\ln(W_{\mathrm{op}})$

We examined the relationship of thermal sensitivity with latitude by fitting regression models with MCMCglmm to all four TPC datasets combined. The response variable was $\ln(E)$ or $\ln(W_{\mathrm{op}})$, whereas possible predictor variables were i) latitude (either in radian units and using a cosine transformation, or as absolute latitude in degree units), ii) the trait from which thermal sensitivity estimates were obtained, and iii) the interaction between latitude and trait identity. To properly incorporate multiple

measurements from the same species (where available), we treated species identity as a random effect on the intercept. We fitted both phylogenetic and non-phylogenetic variants of all candidate models. Two chains per model were run for five million generations each, with samples from the posterior being captured every thousand generations. We verified that each pair of chains had sufficiently converged, after discarding samples from the first 500,000 generations. To identify the most appropriate model, we first rejected models that had a non-intercept coefficient with a 95% Highest Posterior Density (HPD) interval that included zero. We then selected the model with the lowest mean DIC value. To report the proportions of variance explained by the fixed effects ($\mathrm{Var}_{\mathrm{fixed}}$), by the random effect ($\mathrm{Var}_{\mathrm{random}}$), or left unexplained ($\mathrm{Var}_{\mathrm{resid}}$), we calculated the marginal and conditional coefficients of determination [72]:

$$R^2_{\mathrm{m}} = \frac{\mathrm{Var}_{\mathrm{fixed}}}{\mathrm{Var}_{\mathrm{fixed}} + \mathrm{Var}_{\mathrm{random}} + \mathrm{Var}_{\mathrm{resid}}}, \tag{4}$$

$$R^2_{\mathrm{c}} = \frac{\mathrm{Var}_{\mathrm{fixed}} + \mathrm{Var}_{\mathrm{random}}}{\mathrm{Var}_{\mathrm{fixed}} + \mathrm{Var}_{\mathrm{random}} + \mathrm{Var}_{\mathrm{resid}}}. \tag{5}$$

Supporting information

S1 Appendix.

Acknowledgments

We thank Iain Colin Prentice for providing comments on an early version of the manuscript. We are also grateful to James Rosindell and Jonathan Lloyd for useful discussions, and the CIPRES Science Gateway [73] for access to computational resources. Species silhouettes were obtained from phylopic.org and are used under the Public Domain license. The images of species in Fig. 1 were graciously provided by Eric Erbe, Christopher Pooley, and the Rocky Mountain National Park, also under the Public Domain license. DGK was supported by a Natural Environment Research Council (NERC) Doctoral Training Partnership (DTP) scholarship (NE/L002515/1). TPS was supported by a Biotechnology and Biological Sciences Research Council (BBSRC) DTP scholarship (BB/J014575/1). SP was supported by NERC grants NE/M004740/1 and NE/M020843/1.

References

1. Collins M, Knutti R, Arblaster J, Dufresne JL, Fichefet T, Friedlingstein P, et al. Long-term Climate Change: Projections, Commitments and Irreversibility. In: Stocker TF, Qin D, Plattner GK, Tignor M, Allen SK, Boschung J, et al., editors. Climate Change 2013: The Physical Science Basis. Contribution of Working Group I to the Fifth Assessment Report of the Intergovernmental Panel on Climate Change. Cambridge, United Kingdom and New York, NY, USA: Cambridge University Press; 2013. p. 1029–1136.

2. Bathiany S, Dakos V, Scheffer M, Lenton TM. Climate models predict increasing temperature variability in poor countries. Sci Adv. 2018;4(5):eaar5809.

3. Angilletta MJ. Thermal adaptation: a theoretical and empirical synthesis. Oxford University Press; 2009.

4. Clarke A. Principles of Thermal Ecology: Temperature, Energy, and Life. Oxford University Press; 2017.

5. Schoolfield R, Sharpe P, Magnuson C. Non-linear regression of biological temperature-dependent rate models based on absolute reaction-rate theory. J Theor Biol. 1981;88(4):719–731.

6. Brown JH, Gillooly JF, Allen AP, Savage VM, West GB. Toward a metabolic theory of ecology. Ecology. 2004;85(7):1771–1789.

7. Gillooly JF, Brown JH, West GB, Savage VM, Charnov EL. Effects of size and temperature on metabolic rate. Science. 2001;293(5538):2248–2251.

8. Gillooly J, Allen A, Savage V, Charnov E, West G, Brown J. Response to Clarke and Fraser: effects of temperature on metabolic rate. Funct Ecol. 2006;20(2):400–404.

9. Allen A, Gillooly J, Brown J. Linking the global carbon cycle to individual metabolism. Funct Ecol. 2005;19(2):202–213.

10. Clarke A, Fraser K. Why does metabolism scale with temperature? Funct Ecol. 2004;18(2):243–251.

11. Clarke A. Is there a universal temperature dependence of metabolism? Funct Ecol. 2004;18(2):252–256.

12. Clarke A. Temperature and the metabolic theory of ecology. Funct Ecol. 2006;20(2):405–412.

13. Farquhar GD, von Caemmerer S, Berry JA. A biochemical model of photosynthetic CO_2 assimilation in leaves of C_3 species. Planta. 1980;149(1):78–90.

14. Dell AI, Pawar S, Savage VM. Systematic variation in the temperature dependence of physiological and ecological traits. Proc Natl Acad Sci U S A. 2011;108(26):10591–10596.

15. Englund G, Öhlund G, Hein CL, Diehl S. Temperature dependence of the functional response. Ecol Lett. 2011;14(9):914–921.

16. Nilsson-Örtman V, Stoks R, De Block M, Johansson H, Johansson F. Latitudinally structured variation in the temperature dependence of damselfly growth rates. Ecol Lett. 2013;16(1):64–71.

17. Pawar S, Dell AI, Savage VM, Knies JL. Real versus artificial variation in the thermal sensitivity of biological traits. Am Nat. 2016;187(2):E41–E52.

18. Michaletz ST. Evaluating the kinetic basis of plant growth from organs to ecosystems. New Phytol. 2018;219(1):37–44.

19. Savva I, Bennett S, Roca G, Jordà G, Marbà N. Thermal tolerance of Mediterranean marine macrophytes: Vulnerability to global warming. Ecol Evol. 2018;8(23):12032–12043.

20. McShea DW. Mechanisms of large-scale evolutionary trends. Evolution. 1994;48(6):1747–1763.

21. Gilchrist GW. Specialists and generalists in changing environments. I. Fitness landscapes of thermal sensitivity. Am Nat. 1995;146(2):252–270.

22. Schaum CE, Buckling A, Smirnoff N, Studholme DJ, Yvon-Durocher G. Environmental fluctuations accelerate molecular evolution of thermal tolerance in a marine diatom. Nat Commun. 2018;9:1719.

23. Padfield D, Yvon-Durocher G, Buckling A, Jennings S, Yvon-Durocher G. Rapid evolution of metabolic traits explains thermal adaptation in phytoplankton. Ecol Lett. 2016;19(2):133–142.

24. Padfield D, Lowe C, Buckling A, Ffrench-Constant R, Student Research Team, Jennings S, et al. Metabolic compensation constrains the temperature dependence of gross primary production. Ecol Lett. 2017;20(10):1250–1260.

25. Schaum CE, Barton S, Bestion E, Buckling A, Garcia-Carreras B, Lopez P, et al. Adaptation of phytoplankton to a decade of experimental warming linked to increased photosynthesis. Nat Ecol Evol. 2017;1(4):0094.

26. García-Carreras B, Sal S, Padfield D, Kontopoulos DG, Bestion E, Schaum CE, et al. Role of carbon allocation efficiency in the temperature dependence of autotroph growth rates. Proc Natl Acad Sci U S A. 2018;115(31):E7361–E7368.

27. Kontopoulos DG, van Sebille E, Lange M, Yvon-Durocher G, Barraclough TG, Pawar S. Phytoplankton thermal responses adapt in the absence of hard thermodynamic constraints; 2018. Available from: bioRxiv:452250. Cited 4 June 2019.

28. Smith TP, Thomas TJH, García-Carreras B, Sal S, Yvon-Durocher G, Bell T, et al.. Metabolic rates of prokaryotic microbes may inevitably rise with global warming; 2019. Available from: bioRxiv:524264. Cited 4 June 2019.

29. Katoh K, Standley DM. MAFFT multiple sequence alignment software version 7: improvements in performance and usability. Mol Biol Evol. 2013;30(4):772–780.

30. Dress AW, Flamm C, Fritzsch G, Grünewald S, Kruspe M, Prohaska SJ, et al. Noisy: identification of problematic columns in multiple sequence alignments. Algorithms Mol Biol. 2008;3(1):7.

31. Hinchliff CE, Smith SA, Allman JF, Burleigh JG, Chaudhary R, Coghill LM, et al. Synthesis of phylogeny and taxonomy into a comprehensive tree of life. P Natl Acad Sci USA. 2015;112(41):12764–12769.

32. Michonneau F, Brown JW, Winter DJ. rotl: an R package to interact with the Open Tree of Life data. Methods Ecol Evol. 2016;7(12):1476–1481.

33. Stamatakis A. RAxML version 8: a tool for phylogenetic analysis and post-analysis of large phylogenies. Bioinformatics. 2014;30(9):1312–1313.

34. Heath TA, Holder MT, Huelsenbeck JP. A Dirichlet process prior for estimating lineage-specific substitution rates. Mol Biol Evol. 2012;29(3):939–955.

35. Drummond AJ, Ho SY, Phillips MJ, Rambaut A. Relaxed phylogenetics and dating with confidence. PLoS Biol. 2006;4(5):e88.

36. Garamszegi LZ. Modern Phylogenetic Comparative Methods and Their Application in Evolutionary Biology: Concepts and Practice. Springer Berlin Heidelberg; 2014.

37. Hadfield JD. MCMC Methods for Multi-Response Generalized Linear Mixed Models: The MCMCglmm R Package. J Stat Softw. 2010;33(2):1–22.

38. Harmon LJ, Schulte JA, Larson A, Losos JB. Tempo and mode of evolutionary radiation in iguanian lizards. Science. 2003;301(5635):961–964.

39. Murrell DJ. A global envelope test to detect non-random bursts of trait evolution. Methods Ecol Evol. 2018;9(7):1739–1748.

40. Mooers AØ, Vamosi SM, Schluter D. Using phylogenies to test macroevolutionary hypotheses of trait evolution in cranes (Gruinae). Am Nat. 1999;154(2):249–259.

41. Elliot MG, Mooers AØ. Inferring ancestral states without assuming neutrality or gradualism using a stable model of continuous character evolution. BMC Evol Biol. 2014;14(1):226.

42. Spiegelhalter DJ, Best NG, Carlin BP, van der Linde A. Bayesian measures of model complexity and fit. J R Stat Soc Series B Stat Methodol. 2002;64(4):583–639.

43. Thomas MK, Kremer CT, Klausmeier CA, Litchman E. A global pattern of thermal adaptation in marine phytoplankton. Science. 2012;338(6110):1085–1088.

44. Araújo MB, Ferri-Yáñez F, Bozinovic F, Marquet PA, Valladares F, Chown SL. Heat freezes niche evolution. Ecol Lett. 2013;16(9):1206–1219.

45. Sunday J, Bennett JM, Calosi P, Clusella-Trullas S, Gravel S, Hargreaves AL, et al. Thermal tolerance patterns across latitude and elevation. Philos Trans R Soc Lond B Biol Sci. 2019;374(1778):20190036.

46. Dell AI, Pawar S, Savage VM. Temperature dependence of trophic interactions are driven by asymmetry of species responses and foraging strategy. J Anim Ecol. 2014;83(1):70–84.

47. Bestion E, García-Carreras B, Schaum CE, Pawar S, Yvon-Durocher G. Metabolic traits predict the effects of warming on phytoplankton competition. Ecol Lett. 2018;21(5):655–664.

48. Pucci F, Rooman M. Physical and molecular bases of protein thermal stability and cold adaptation. Curr Opin Struct Biol. 2017;42:117–128.

49. Thomas MK, Aranguren-Gassis M, Kremer CT, Gould MR, Anderson K, Klausmeier CA, et al. Temperature–nutrient interactions exacerbate sensitivity to warming in phytoplankton. Glob Chang Biol. 2017;23:3269–3280.

50. Bestion E, Schaum CE, Yvon-Durocher G. Nutrient limitation constrains thermal tolerance in freshwater phytoplankton. Limnol Oceanogr Lett. 2018;3(6):436–443.

51. Rohr JR, Civitello DJ, Cohen JM, Roznik EA, Sinervo B, Dell AI. The complex drivers of thermal acclimation and breadth in ectotherms. Ecol Lett. 2018;21(9):1425–1439.

52. Wang H, Atkin OK, Keenan TF, Smith N, Wright IJ, Bloomfield KJ, et al.. Thermal acclimation of leaf respiration consistent with optimal plant function; 2018. Available from: bioRxiv:434084. Cited 4 June 2019.

53. Somero GN. Proteins and temperature. Annu Rev Physiol. 1995;57(1):43–68.

54. Hobbs JK, Jiao W, Easter AD, Parker EJ, Schipper LA, Arcus VL. Change in heat capacity for enzyme catalysis determines temperature dependence of enzyme catalyzed rates. ACS Chem Biol. 2013;8(11):2388–2393.

55. DeLong JP, Gibert JP, Luhring TM, Bachman G, Reed B, Neyer A, et al. The combined effects of reactant kinetics and enzyme stability explain the temperature dependence of metabolic rates. Ecol Evol. 2017;7(11):3940–3950.

56. Cooper BS, Hammad LA, Montooth KL. Thermal adaptation of cellular membranes in natural populations of *Drosophila melanogaster*. Funct Ecol. 2014;28(4):886–894.

57. Braakman R, Follows MJ, Chisholm SW. Metabolic evolution and the self-organization of ecosystems. Proc Natl Acad Sci U S A. 2017;114(15):E3091–E3100.

58. Finlay BJ. Global dispersal of free-living microbial eukaryote species. Science. 2002;296(5570):1061–1063.

59. Tamames J, Abellán JJ, Pignatelli M, Camacho A, Moya A. Environmental distribution of prokaryotic taxa. BMC Microbiol. 2010;10(1):85.

60. Doblin MA, van Sebille E. Drift in ocean currents impacts intergenerational microbial exposure to temperature. Proc Natl Acad Sci U S A. 2016;113(20):5700–5705.

61. Johnston ASA, Sibly RM. The influence of soil communities on the temperature sensitivity of soil respiration. Nat Ecol Evol. 2018;2(10):1597–1602.

62. Tavaré S. Some probabilistic and statistical problems in the analysis of DNA sequences. In: Miura RM, editor. Some Mathematical Questions in Biology: DNA Sequence Analysis. Providence (RI): American Mathematical Society; 1986. p. 57–86.

63. Gu X, Fu YX, Li WH. Maximum likelihood estimation of the heterogeneity of substitution rate among nucleotide sites. Mol Biol Evol. 1995;12(4):546–557.

64. Pattengale ND, Alipour M, Bininda-Emonds OR, Moret BM, Stamatakis A. How many bootstrap replicates are necessary? In: Annual International Conference on Research in Computational Molecular Biology. Springer; 2009. p. 184–200.

65. Gelman A, Rubin DB. Inference from iterative simulation using multiple sequences. Stat Sci. 1992;7(4):457–472.

66. Brooks SP, Gelman A. General methods for monitoring convergence of iterative simulations. J Comput Graph Stat. 1998;7(4):434–455.

67. Rambaut A, Drummond AJ. TreeAnnotator; 2018 [cited 30 November 2018]. Available from: `http://beast.community/treeannotator`.

68. Kontopoulos DG, García-Carreras B, Sal S, Smith TP, Pawar S. Use and misuse of temperature normalisation in meta-analyses of thermal responses of biological traits. PeerJ. 2018;6:e4363.

69. Oehlert GW. A note on the delta method. Am Stat. 1992;46(1):27–29.

70. Thomas GH, Freckleton RP. MOTMOT: models of trait macroevolution on trees. Methods Ecol Evol. 2012;3(1):145–151.

71. Puttick M, Thomas G, Freckleton R, Ingram T, Orme D, Paradis E. motmot.2.0: Models of Trait Macroevolution on Trees; 2018.

72. Nakagawa S, Schielzeth H. A general and simple method for obtaining R^2 from generalized linear mixed-effects models. Methods Ecol Evol. 2013;4(2):133–142.

73. Miller MA, Pfeiffer W, Schwartz T. Creating the CIPRES Science Gateway for inference of large phylogenetic trees. In: Gateway Computing Environments Workshop (GCE), 2010. Ieee; 2010. p. 1–8.